Global Change Biology

Global Change Biology (2010) **16**, 1589–1605, doi: 10.1111/j.1365-2486.2009.02111.x

Multiscale analysis of temporal variability of soil CO_2 production as influenced by weather and vegetation

RODRIGO VARGAS*, MATTEO DETTO*, DENNIS D. BALDOCCHI* and MICHAEL F. ALLEN†

*Department of Environmental Science, Policy and Management, Ecosystem Sciences Division, University of California, Berkeley, CA 94720, USA, †Center for Conservation Biology, University of California, Riverside, CA 92521, USA

Abstract

Ecosystem processes are influenced by weather and climatic perturbations at multiple temporal scales with a large range of amplitudes and phases. Technological advances of automated biometeorological measurements provide the opportunity to apply spectral methods on continuous time series to identify differences in amplitudes and phases and relationships with weather variation. Here we used wavelet coherence analysis to study the temporal covariance between soil CO_2 production and soil temperature, soil moisture, and photosynthetically active radiation (PAR). Continuous (hourly average) data were acquired over 2 years among three vegetation types in a semiarid mixed temperate forest. We showed that soil temperature and soil moisture influence soil CO_2 production differently at multiple periods (e.g. hours, days, weeks, months, years), especially after rain pulse events. Our results provide information about the periodicity of soil CO_2 production among vegetation types, and provide insights about processes controlling CO_2 production through the study of phase relationships between two time series (e.g. soil CO_2 production and PAR). We tested the performance of empirical models of soil CO_2 production using the continuous wavelet transform. These models, built around soil temperature and moisture, failed at multiple periods across the measured dates, suggesting that empirical models should include other factors that regulate soil CO_2 production at different temporal scales. Our results add a new dimension for the analysis of continuous time series of biometeorological measurements and model testing, which will prove useful for analysis of increasing sensor data obtained by environmental networks.

Keywords: CO_2 sensors, model performance, rain pulse, soil respiration, temperature independent, time series analysis, wavelet analysis, wavelet coherence, wireless sensors

Received 18 May 2009; revised version received 7 September 2009 and accepted 1 October 2009

Introduction

Emissions of CO_2 from soils (i.e. CO_2 efflux, R_s) represent a major flux of carbon into the atmosphere (Raich & Potter, 1995), and climate records indicate that the Earth is experiencing important biophysical changes (Hughes, 2000) with an overall trend of increasing temperatures for the past 100 years (IPCC, 2007). Changes in precipitation and temperature may influence the interannual variability of R_s (Raich *et al*., 2002), and changes in vegetation distribution will affect carbon dynamics at the landscape scale (Bachelet *et al*., 2001; Lenihan *et al*., 2003). Thus, it is crucial to understand how climate and weather variability influences R_s, and which biophysical factors drive R_s in different vegetation types.

The general pattern of climate change models suggests that southern California and northern Mexico are persistent hotspots for changes in interannual climate variability (Diffenbaugh *et al*., 2008). The California mixed conifer forest is like many semiarid forest regions in that it is composed of patches of trees and small meadows. In many cases, the meadow patches are actually small burns resulting from lightning strikes burning small tree stands, or smoldering fires burning understory and small tree patches. Today, these dynamics have changed and the relative amounts of meadow and forest are being altered in an unpredictable manner. Fires and climate variation in these mixed forests have affected species composition, forest structure, and forest function (Minnich *et al*., 2000; Lenihan

Correspondence: Rodrigo Vargas, tel. + 1 510 642 2421, fax 1 510 643 5098, e-mail: rvargas@berkeley.edu

et al., 2003; Battles et al., 2008). Expected climate change may influence species composition and interannual variation in temperature and precipitation in semiarid forests, thus it is crucial to understand the influence of biophysical factors on R_s at multiple spatial and temporal scales.

R_s is the result of production of CO_2 in the soil (P_s) by autotrophic (roots and mycorrhizae) and heterotrophic (decomposers) respiration processes (Hanson et al., 2000; Ryan & Law, 2005). Variation of P_s in the soil profile changes soil CO_2 concentration gradients, and in conjunction with changes in soil CO_2 diffusivity these biophysical processes regulate R_s (Šimůnek & Suarez, 1993). While previous studies have focused on R_s in multiple biomes and vegetation types (e.g. Ryan & Law, 2005), a mechanistic description of soil CO_2 dynamics is needed to understand how P_s may vary in relation to weather and climate variation (Davidson & Trumbore, 1995; Hashimoto & Suzuki, 2002). The importance of P_s relies on the fact that it is directly related to the biological activity in the soil, while R_s provides integrated information about the interaction between soil structure, biophysical dynamics, and the atmosphere.

Automated continuous measurements of R_s (see Goulden & Crill, 1997; Savage & Davidson, 2003) provide insights about processes, which were not possible to explore before. For example, one can identify phase lags between R_s and soil temperature, at diel (Tang et al., 2005; Gaumont-Guay et al., 2006; Riveros-Iregui et al., 2007; Bahn et al., 2008; Vargas & Allen, 2008a) and seasonal scales (Moren & Lindroth, 2000; Drewitt et al., 2002; Vargas & Allen, 2008b), and previous studies have identified responses of R_s to diel temperature independence (Liu et al., 2006; Vargas & Allen, 2008c), rain pulses (Jassal et al., 2005; Daly et al., 2008), and changes in the influence of soil temperature and soil moisture on R_s (Goulden & Crill, 1997; Irvine & Law, 2002; Carbone et al., 2008). However, with increasing numbers and length of continuous measurements of biometeorological variables (e.g. soil CO_2 efflux) it is important to identify alternative tools to analyze the dependencies between these series and the series of the environmental factors (e.g. temperature and soil moisture).

Ecosystem processes are influenced by weather and climatic perturbations, which often contain oscillations at multiple temporal scales (Baldocchi et al., 2001; Bowling et al., 2002). We propose that complex spectral methods are needed to better understand the temperature and water dependence of soil CO_2 processes. Previous studies have used Fourier transform (Tang et al., 2005; Baldocchi et al., 2006) and cross-correlation (Stoy et al., 2007) analysis to investigate spectral properties of soil CO_2 signals. However, these analyses failed in presence of nonstationary phenomena (Katul et al., 2001a) such as a rain pulses, heat waves, or freezing events. Soil CO_2 signals (and most biometeorological measurements) typically violate the stationary assumption underlying the analysis of 'global' spectral properties. Moreover, as many meteorological variables, these signals contain strong periodicities that further complicate their interpretation. Here, we use the continue wavelet transform as a novel approach to the interpretation of soil CO_2 time series, where smooth, continuous variations in wavelet amplitude are expected (Torrence & Compo, 1998).

Wavelet transforms originated in geophysics in the early 1980s for the analysis of seismic signals. Since then, this technique has been applied in many other scientific fields including for analysis of meteorological data (Farge, 1992; Collineau & Brunet, 1993; Gao & Li, 1993; Kumar & Foufoula Georgiou, 1997; Torrence & Webster, 1999; Grinsted et al., 2004), but has rarely been applied to study time series of biophysical measurements such as fluxes of CO_2 and water vapor between ecosystem and atmosphere (Katul et al., 2001b; Stoy et al., 2005). Detailed reviews on the application and theory of wavelet analysis can be found in many studies (Farge, 1992; Torrence & Compo, 1998; Grinsted et al., 2004; Cazelles et al., 2008). The advantage of wavelet analysis over other time series analysis is that the window size is not fixed, varying as a function of frequency with an optimal trade-off between time and frequency resolution overcoming the problems of nonstationarity in time series. The intrinsic smoothing property of the wavelet produces results that are more easily interpretable, without the need of excessive manipulation of the original signal (e.g. averaging, smoothing, and tapering) or without restrictive assumptions (e.g. periodicity, stationarity). Furthermore, wavelet analysis can be performed in two time series of biophysical interest (e.g. soil CO_2 production and temperature) and can provide information of causality through analysis of the phase relationship between these two time series (e.g. cross-wavelet transform, wavelet coherence analysis) (Grinsted et al., 2004; Govindan et al., 2005).

The main goal of this study was to test how the temporal covariance between P_s and soil temperature, and soil moisture changed among three adjacent vegetation types in a semiarid mixed temperate forest in Southern California. We compared the variation in measurements collected from January 2006 to February 2008. The studied vegetations were in a short distance (<150 m) and represent a transition between mature mixed forest and an open meadow with similar soil properties and meteorological conditions (Vargas & Allen, 2008b). Thus, this experimental design allowed us to explore how different vegetation types respond to

similar weather variations. The specific objectives were (1) to apply wavelet coherence analysis as a novel approach for soil CO_2 research using hourly measurements of P_s, soil temperature, soil moisture, and photosynthetically active radiation (PAR). Using this technique we propose that it is possible to infer additional information about the biophysical processes that regulate soil CO_2 fluxes by examining the temporal patterns and relationships (i.e. phase differences) among these variables. (2) To use wavelet analysis to test the performance of empirical models among vegetation types and identified periods (e.g. hours, days, months) and time domains (i.e. day of the year) where the models fail. Empirical models with soil temperature and soil water content have been widely used to represent variation in R_s (Davidson *et al.*, 1998; Reichstein *et al.*, 2003; Ryan & Law, 2005), but they may not accurately represent the variation of soil CO_2 fluxes at multiple periods along the time domain (i.e. days of the year).

In this study we tested the following hypotheses:

H1: P_s has a spectral signature with a strong signal at the 1-day and 1-year (~360 days) periods at all vegetation types, but the spectral signature at intermediate scales (weeks–months) may vary among them.

The pattern of solar radiation at the 1-day (variation in day and night) and at 1-year period (seasonal variation) influences plant photosynthesis and microbial heterotrophic metabolism. At intermediate scales plant phenology and weather patterns (e.g. cold periods, heat waves, or rain pulses) that influence soil moisture and soil temperature could differentially influence plant and microbial activity among vegetation types. Multiple studies have investigated the influence of these transient events in soil CO_2 fluxes at intermediate temporal scales (Schimel & Clein, 1996; Huxman *et al.*, 2004; Jarvis *et al.*, 2007) and here we explored their influence in the spectral characteristics of P_s.

H2: The phase differences between two time series, within a specific period (e.g. 1 day), could provide insights of the timing of mechanisms that regulate soil CO_2 fluxes.

The phase differences could be seen as the temporal lag between two time series within a specific period and can provide information of causality between two processes (Grinsted *et al.*, 2004). Therefore, we explore if changes in the P_s time series occur at the same time (in phase with no lags) as changes in the soil temperature or PAR, or is there a tendency for changes in P_s to lag (out of phase) behind or ahead changes in the other time series.

Methods

Study site

The study was conducted at the University of California James San Jacinto Mountain Reserve, a UC Natural Reserve System field station. The Reserve is a mixed conifer-oak forest at 1640 m.a.s.l. located in the San Jacinto Mountains, CA, USA (33°48′30″N, 116°46′40″W). Most of the precipitation occurs between the months of November and April with a mean annual precipitation of 640 mm and a mean air temperature of 10.3 °C. The Reserve serves as the Terrestrial Ecology Observing Systems field site for the Center for Embedded Networked Sensing (CENS, http://cens.ucla.edu) with the goals to research and develop new wireless environmental-sensing technologies for ecological observations (Allen *et al.*, 2007).

In October 2005 we established a 150 m transect from an area of mature woody vegetation, passing through an area of young woody vegetation, and ending in an adjacent open meadow with scattered herbaceous vegetation (Vargas & Allen, 2008b). These transitions are becoming more abundant in these mixed forests due to recurrent fires and climate variation (e.g. long-term droughts). The vascular plants present at mature woody vegetation were large individuals (DBH > 30 cm) of *Quercus chrysolepis* Leibem. (Canyon live oak), and *Pinus ponderosa* C. Lawson (Ponderosa Pine). The vascular plants present at young woody vegetation were medium individuals (DBH < 20 cm) individuals of *Quercus kelloggii* Newb. (California black oak), *Calocedrus decurrens* (Torr.) Florin (Incense cedar), *Arctostaphylos pringlei* Parry (Manzanita), and *Pinus lambertiana* Dougl. (Sugar pine). The scattered herbaceous vegetation at the meadow included individuals of *Eriogonum wrightii* Torr. Ex Benth (Bastard sage) of < 10 cm in height and a density of nearly 2 plants m^{-2}. Bastard sage was also present at the understory of young woody vegetation with a similar density as at scattered herbaceous vegetation meadow. Soils had similar physical characteristics (Table 1) and fine root biomass (< 2 mm in diameter) was low in the scattered herbaceous meadow (10 g m^{-2}), medium in young woody vegetation (18 g m^{-2}), and high in mature woody vegetation (25 g m^{-2}).

Soil CO_2 measurements

Along the 150 m transect we established one 40 m^2 plot for each vegetation type. Within these plots, we installed a suite of soil wireless sensors (i.e. nodes) to monitor gas-phase CO_2 concentrations (CARBOCAP, GMM 222, Vaisala, Helsiniki, Finland), temperature

Table 1 Soil characteristics and fine root biomass at three vegetation types at the James Reserve, a mixed temperate forest in Southern California, USA

Site	Soil carbon (%)	Nitrogen (%)		Fine root biomass ($g\,m^{-2}$)	Soil bulk density ($g\,cm^{-3}$)	Soil texture (%)		
		Soil	Fine roots			Sand	Silt	Clay
MWv	3.3 (0.5)	0.07 (0.05)	0.64 (0.29)	25 (2.32)	0.79 (0.2)	83	10	7
YWv	3.1 (0.5)	0.08 (0.02)	0.58 (0.23)	18 (1.56)	0.85 (0.3)	83	10	7
Hv	2.4 (0.5)	0.05 (0.03)	0.53 (0.24)	10 (2.75)	1.2 (0.1)	83	10	7

Numbers in parentheses represent $\pm$ 1 SD.
MWv, mature woody vegetation; YWv, young woody vegetation; Hv, scattered herbaceous meadow.

and moisture (Decagon, ECHO) simultaneously at several depths in the soil (2, 8, 16 cm) as described previously (Allen *et al*., 2007; Vargas & Allen, 2008b). At young woody vegetation and scattered herbaceous meadow we installed four nodes, and at mature woody vegetation two nodes for a total of 30 CO_2 sensors in a replicated design. The CO_2 sensors were protected with Gore-Tex® fiber to avoid possible wetting during rainfall events and calibrated every 6 months against reference gases. Measurements were recorded every 5 min and averaged every hour from January 2006 to February of 2008.

Soil CO_2 fluxes were calculated using the flux gradient method described previously (Vargas & Allen, 2008b) with modifications for signal processing and calculation of P_s. Briefly, the CO_2 concentration from the sensors was corrected for temperature and pressure accordingly to the manufacturer (Vaisala, Helsiniki, Finland). We applied a Savitzky–Golay smoothing filter, which preserves peak heights and widths of the original signal to reduce noise of measured CO_2 concentrations. A similar approach was used by Chen *et al*. (2005) for continuous measurements of CO_2 concentrations using a cubic polynomial and a frame size of 8. These corrected CO_2 concentrations were used to calculate the flux of CO_2 between any two layers at depth *i*th in the soil profile using Fick's law of diffusion. Diffusivity of soil CO_2 in the soil profile was calculated using the Moldrup model (Moldrup *et al*., 1999), which is based on diffusion through porous media:

$$\frac{D_s}{D_a} = \phi^2 \left(\frac{\varepsilon}{\phi}\right)^{\beta S}, \quad (1)$$

where D_s is the gaseous CO_2 diffusion coefficient in the soil, D_a the CO_2 molecular diffusivity of CO_2 in the air, β is a constant ($\beta = 2.9$), S = silt + sand content ($S = 93$), and ϕ is soil porosity (see Vargas & Allen, 2008b, c). Assuming a constant rate of CO_2 production in the soil profile, R_s can be calculated as

$$R_s = \frac{z_{i+1}F_i - z_i F_{i+1}}{z_{i+1} - z_i}, \quad (2)$$

where F_i, and F_{i+1} are CO_2 effluxes ($\mu mol\,m^{-2}\,s^{-1}$) at depths z_i and z_{i+1} (m), respectively. The storage term was negligible at these depths for our study site, and the condition of constant CO_2 production throughout the soil profile may not be entirely met in productive ecosystems where soil CO_2 storage may be changing. Fluxes calculated using the flux gradient method and the Moldrup model for soil CO_2 diffusivity have been extensively validated with the chamber flux method (LI-8100, LI-COR Lincoln, NE, USA) at the study site showing good agreement (Vargas & Allen, 2008b, c).

To estimate soil CO_2 production (P_s) first we estimated F_i at two depths between 0.02–0.08 and 0.08–0.16 m. Once F_i was calculated for discrete layers in the soil profile, P_s was calculated from the difference between the effluxes across soil layers as a flux divergence (Šimůnek & Suarez, 1993):

$$P_s = \frac{F_i - F_{i+1}}{z_{i+1} - z_i}, \quad (3)$$

where P_s is soil CO_2 production ($\mu mol\,m^{-3}\,s^{-1}$) at depth ($z_{i+1} - z_i$) or 8.5 cm depth for this case. We report hourly averages of P_s as positive values. We averaged time series of multiple nodes at the same vegetation to report a mean time series per vegetation type.

Wavelet analysis

Previous works have reviewed in detail the concepts of wavelet analysis for different applications (Daubechies, 1990; Torrence & Compo, 1998; Cazelles *et al*., 2008). Here, we list some important concepts with special attention to some properties used in this study.

The wavelet transform of a discrete signal x_n of length N recorded at δt interval, is defined as the convolution integral

$$W_n(s) = \left(\frac{\delta t}{s}\right)^{1/2} \sum_{n'=0}^{N-1} x_{n'}\, \psi_0^* \left(\frac{n - n'}{s/\delta t}\right), \quad (4)$$

where ψ_0^* is the complex conjugate of the scaled and translated mother wavelet and s is the wavelet scale at which the transform is applied. The continuous wavelet

transform is calculated by continuously shifting the scale and time in Eqn (4). The mother wavelet with all its dilations and translations form an over-complete basis of N^2 coefficients. Thus, there is redundant information in the coefficients of the wavelet transform as they are not independent. The continuous wavelet transform can be viewed as a microscope able to reveal details of the signal at the position n with the magnification s. This approach is useful for time series analysis, where the power of the signal is modulated at different scales and it varies with time. For this study we used the continuous wavelet transform because of its ability to produce a smooth picture in time-scale domain of a nonstationary process (i.e. soil CO_2 production) and it is suitable for visual interpretation.

The ability to discern small intervals of scales (spectral resolution), depends on the choice of the wavelet because wavelets with good frequency resolution have poor time localization (temporal resolution) and vice versa ('Heisenberg principle'). One of the most-used mother wavelets for geophysical applications is the Morlet wavelet (Torrence & Webster, 1999; Grinsted *et al*., 2004), given by

$$\psi_0 = \pi^{-1/4} e^{i\omega_0 t} e^{-t^2/2}, \tag{5}$$

where ω_0 (the base frequency) is set to 6. The Morlet is a complex nonorthogonal wavelet with a good time and scale resolution. A complex wavelet function, such as this, has the advantage to return information about both amplitude and phase.

The cross-wavelet transform of two time series, $x = [x_n]$ and $y = [y_n]$, at scale s, first introduced by Hudgins *et al*. (1993) is defined as

$$W_n^{xy}(s) = W_n^x(s) W_n^{y*}(s), \tag{6}$$

where $W_n^{y*}(s)$ is the complex conjugate of $W_n^y(s)$. The cross-wavelet amplitude is given then by $\left|W_n^{xy}(s)\right|$, while the phase difference is defined as $\tan^{-1}\left[\Im\{W_n^{xy}(s)\}/\Re\{W_n^{xy}(s)\}\right]$. Here, $\Im$ represents the imaginary part and $\Re$ is the real part of $W_n^y(s)$. The cross-wavelet transform is simply the bivariate extension of the wavelet analysis and is used to explore the relationship between two time series to expose their common power in frequency domain (Grinsted *et al*., 2004).

The wavelet coherence analysis is defined as

$$\mathrm{WCA(s)} = \frac{\left|\left\langle s^{-1} W_n^{xy}(s)\right\rangle\right|^2}{\left|\left\langle s^{-1} W_n^{x}(s)\right\rangle\right|^2 \left|\left\langle s^{-1} W_n^{y}(s)\right\rangle\right|^2}, \tag{7}$$

where the angular brackets indicate a smoothing in time and scale. As in Fourier analysis, it is necessary to smooth the spectra and the cross spectrum before calculating coherency (which is otherwise identically equal to 1). The smoothing is performed in both, time and scale using the method proposed by Torrence & Webster (1999), which provides the minimal amount of smoothing necessary to include two independent points in both dimensions. Wavelet coherence analysis is similar to the cross-wavelet transform and can be thought of as the local correlation, between two time series. Importantly, wavelet coherence analysis finds regions in time–frequency space where two time series covary but do not necessarily have high common power (Grinsted *et al*., 2004; Cazelles *et al*., 2008).

In this study we focused on wavelet coherence analysis instead of the cross-wavelet transform for several reasons (1) there is some redundancy between the two measurements but they are complementary, (2) the wavelet coherence analysis reveals correlations in regions of the frequency domain where the two variables do not necessarily have high common power, and (3) there is evidence that the cross-wavelet transform may not be the best approach for significance testing of the interrelation between two time series (Maraun & Kurths, 2004), but the choice of a stationary test can be challenging (Lau & Weng, 1995). One of the reasons is that entire subsets of the record may be dropped below the significant level, due to the intrinsic nonstationarity of the process. Wavelet coherence analysis partially avoids this problem because in each region the copower is normalized by the local power of the two time series [Eqn (7)]. Although we only present the wavelet coherence analysis, our interpretations of the results and discussion are based on both wavelet coherence analysis and cross-wavelet transform.

The statistical significance (5% significance level) of common power between two time series (e.g. soil CO_2 production and soil temperature) was assessed within the cone of influence of the wavelet coherence analysis using Monte Carlo simulations of wavelet coherency between 10 000 sets (two each) of white noise time series (Torrence & Webster, 1999). Grinsted *et al*. (2004) showed that the color of the noise has little impact on the 5% significance level analysis. The cone of influence is the region in which the wavelet transform suffers from edge effects because of incomplete time-locality across frequencies (Torrence & Compo, 1998), thus outside the cone of influence the results are unreliable and have to be interpreted carefully. To reduce errors at the beginning and at the end of the wavelet power spectrum the time series were padded with zeros which introduces discontinuities at endpoints and therefore it is important to be aware of edge effects delimited by the cone of influence in the wavelet spectrum (Torrence & Compo, 1998).

The phase relationships, which can be expressed in unit of time multiplying by the respective period, inform on synchronization between oscillations of the two time series (Govindan *et al*., 2005). The delay between

two time series can provide information on the nature and origin of coupling between the processes, and causality under the assumption that the effect must follow the cause. Here we calculated the mean phase difference between P_s and soil temperature or PAR (as a surrogate for photosynthesis) at the 1-day period to explore H2. Furthermore, we tested the influence of soil temperature measurement depth on the mean phase difference at the 1-day period for P_s and soil temperature to explore the influence of heat transfer in the soil.

We applied the wavelet coherence analysis to the sets of hourly time series of P_s, soil temperature at depth of P_s, soil moisture, or PAR previously normalized. Data analyses were performed using MATLAB R2007a (The MathWorks Inc.), and wavelet analysis software written by C. Torrence (ITT Visual Info. Solutions, Boulder, CO, USA), G. P. Compo (NOAA/CIRES Climate Diagnostics Center, Boulder, CO, USA) and A. Grinsted (Arctic Centre, University of Lapland, Finland).

Soil CO_2 production modeling and spectral testing

We tested two empirical models for P_s at three vegetation types using hourly means of the variables involved. The first model was a simple exponential equation with soil temperature as an independent variable:

$$P_s = B_1 e^{(B_2 T)}. \quad (8)$$

The second model was a combination of soil temperature and volumetric water content and has been used in semiarid ecosystems where changes in soil temperature and water are important drivers for P_s (Xu *et al*., 2004; Vargas & Allen, 2008c):

$$P_s = B_1 e^{(B_2 T)} e^{(B_3\theta)+(B_4\theta^2)}, \quad (9)$$

where P_s is soil CO_2 production ($\mu mol\ CO_2\ m^{-3}\ s^{-1}$), T is soil temperature (°C) at depth of P_s, θ is soil water content ($m^3\ m^{-3}$, average 2–16 cm depth), and B_0–B_4 are model parameters estimated using the Levenberg–Marquardt method. To select the best statistical model for P_s, we used the root mean squared error (RMSE), and the Akaike Information Criterion (AIC) as a penalized likelihood criterion (Burnham & Anderson, 2002):

$$AIC = -2\ln(L) + 2p, \quad (10)$$

where L is the likelihood of the fitted model, and p is the total number of parameters in the model. The best statistical model minimizes the value of AIC.

Once the best statistical model for P_s was selected, we used the continuous wavelet power spectrum of the residuals of that model to identify significant regions in the spectral signature where the model fails. This approach allowed testing model performance at multiple periods and time domains, as we can identify patters where the signal of the residuals is large (i.e. large variation in residuals means poor model fit).

Results and discussion

Our results showed how the temporal covariance between soil temperature and soil moisture with soil CO_2 production (P_s) changed at multiple periods (e.g. hours, days, weeks, months, years) along the time domain (i.e. days of the year) among adjacent vegetation types in a semiarid mixed temperate forest. We propose that wavelet coherence analysis of continuous time series is a useful statistical tool to understand interactions among biophysical factors and provide insights about the periodicity of processes that regulate P_s under weather variation. Furthermore, we tested empirical models using continuous wavelet transform and showed that these models failed to represent soil CO_2 fluxes at multiple periods among vegetation types.

We analyzed over 2 years of measurements where the first year was characterized as a warmer but slightly wetter year (Table 1), with high precipitation during spring that substantially increased soil moisture (Fig. 1). In contrast, the second year was slightly colder (Table 1) with lower and less variable soil moisture content during winter and spring (Fig. 1). Although all vegetation types were exposed to the same meteorological conditions, they had slightly different patterns in interannual soil temperature and soil moisture (Fig. 1). In general, the mature woody vegetation was slightly warmer and the soils were moister than the other vegetation types likely because of higher canopy cover that intercepted rainfall and reduced soil evaporation. We were able to detect two summer rainfall events (Fig. 1; days 200 and 630 after January 1, 2008), where the effects on soil water content were different between years and among vegetation types (Fig. 1). Summer rainfalls are critical because they are drivers for soil microbial processes (Fierer *et al*., 2003; Collins *et al*., 2008), biological activity (Potts *et al*., 2006), and soil CO_2 pulses at the study site (Vargas & Allen, 2008b) and other arid and semiarid ecosystems (Huxman *et al*., 2004; Xu *et al*., 2004; Jarvis *et al*., 2007).

Different interannual patterns of soil temperature and soil moisture had a large effect on the timing and patterns of P_s. Our observations showed that, during the first year, spring rainfall was associated with higher fluxes and higher variation of P_s in comparison with the drier following year (Fig. 2). We observed a reduction in mean annual P_s (and R_s) at the mature woody vegetation and scattered herbaceous meadow from the first to the second year, but an increase at the young woody vegetation (Fig. 2, Table 2). By studying the measured variables in the time domain, it is clear that rain pulses

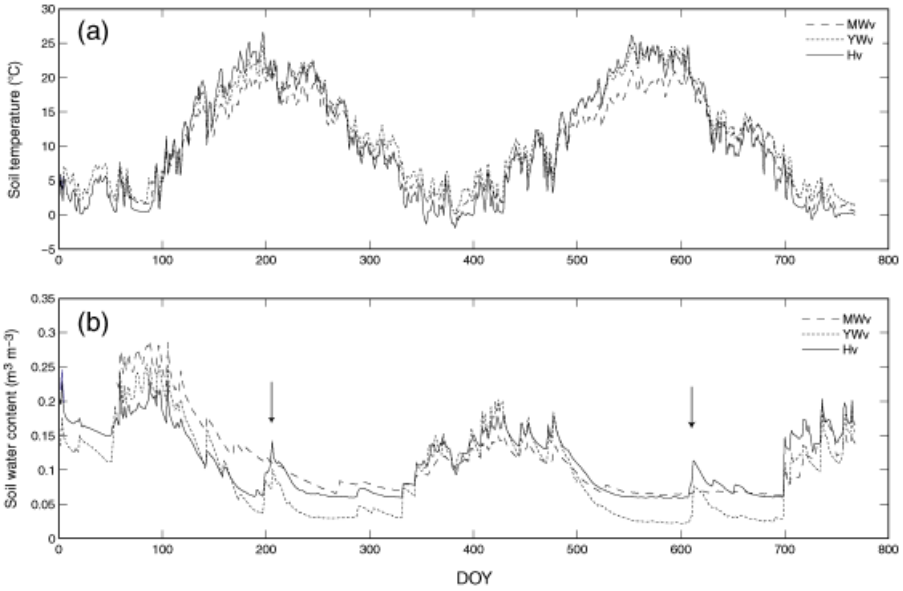

Fig. 1 Seasonal trends of (a) soil temperature and (b) soil moisture at the James San Jacinto Mountains Reserve from January 2006 to February 2008 at three vegetation types. The time series represents DOY after January 1, 2006. DOY, day of the year; MWv, mature woody vegetation; YWv, young woody vegetation; Hv, scattered herbaceous meadow. Arrows indicate the approximate date of summer rainfall events.

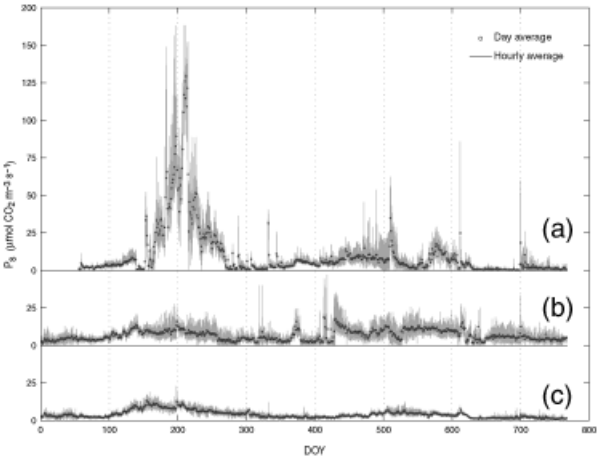

Fig. 2 Hourly and daily means of soil CO_2 production (P_s) at (a) mature woody vegetation, (b) young woody vegetation, and (c) scattered herbaceous meadow from January 2006 to February 2008. DOY, day of the year after January 1, 2006.

and rapid changes in soil temperature are transient events that influence patterns of P_s among vegetation types (Figs 1 and 2). Next we explored the spectral characteristics of these irregular and nonstationary time series to extract information from their frequency domains that could provide insights of the periodicity at which different processes may regulate soil CO_2 fluxes.

Periodicity of soil CO_2 production, temperature, soil moisture

The control of soil CO_2 fluxes by soil temperature and soil water content is well documented in different ecosystems (Davidson *et al*., 2000; Curiel Yuste *et al*., 2003; Reichstein *et al*., 2003), but by studying the time series in the frequency domain one can identify the main periodic components. First, we studied the global wavelet power spectrum (Fig. 3), which is defined as the averaged variance contained in all wavelet coefficients of the same frequency and provides quantification of the main periodic components of a time series (Torrence & Compo, 1998).

The global power spectrum of soil temperature showed a strong periodicity at the 1-day and 1-year, while the global power spectrum of soil moisture had a strong periodicity at intermediate scales (weeks to months) and 1-year (Fig. 3a). Variation in soil moisture at weeks and months was a result of seasonal precipitation events (Fig. 1). Similarly, the global power spectrum of P_s showed the expected pronounced peaks at 1-day and 1-year periods for all vegetation types (Fig. 3b). This pattern is common to most biological processes because they respond to diel and seasonal variations of meteorological phenomena of changes in temperature. Differences at the 1-year period among vegetation types were likely a result of stochastic fluctuations due to site differences, and these fluctuations

Table 2 Mean values divided by measurement years of soil temperature, air temperature, soil moisture, soil CO_2 production (*Ps*), and soil respiration (*Rs*)

Variable	Depth	MWv	YWv	Hv
Soil temperature (°C)				
Mean of 2 years	2 cm	10.8	11.1	10.9
Mean of 2 years	8 cm	10.5	11.8	10.6
Mean of 2 years	16 cm	10.3	11.6	10.5
Air temperature (°C)				
Mean of 2 years		9.7	9.4	9.4
Mean year 1		9.5	9.6	9.6
Mean year 2		9.2	9.3	9.3
Soil moisture ($m^3\,m^{-3}$)				
Mean of 2 years		0.11	0.10	0.11
Mean year 1		0.13	0.11	0.11
Mean year 2		0.09	0.08	0.10
Ps ($\mu mol\,CO_2\,m^3\,s^{-1}$)				
Mean of 2 years		18.7	13.6	8.3
Mean year 1		28.0	12.2	11.0
Mean year 2		10.4	14.9	6.0
Rs ($\mu mol\,CO_2\,m^2\,s^{-1}$)				
Mean of 2 years		2.2	2.1	1.1
Mean year 1		2.7	2.0	1.3
Mean year 2		1.9	2.1	0.8
Rs sum ($gC\,m^2\,yr^{-1}$)				
Mean of 2 years		1130	797	539
Year 1		1171*	763	524
Year 2		1090	831	555

*Measurements of 50 days were missing at MWv during the beginning of the first year.
Hv, scattered herbaceous meadow; MWv, mature woody vegetation; YWv, young woody vegetation.

may influence the interannual response of the autotrophic and heterotrophic components of P_s among vegetation types.

The global power spectrum showed that the spectral characteristics of P_s varied among vegetation types at intermediate periods (e.g. weeks–months) supporting H1. Possible factors that regulate P_s at these periods are different responses of microbes (Fierer *et al*., 2003) and vegetation (Xu *et al*., 2004) to water and temperature pulses, site variation in plant phenology (DeForest *et al*., 2006), differences in canopy photosynthesis (Baldocchi *et al*., 2006; Irvine *et al*., 2008), and differences in root and rhizomorph dynamics (Vargas & Allen, 2008a). Our results are consistent with previous findings that have identified strong periodicities in biometeorological measurements at similar intermediate periods (Baldocchi *et al*., 2001), and these results support the importance of understanding biophysical factors that may influence interannual variability of ecosystem CO_2 fluxes (Mahecha *et al*., 2007). The fact that P_s (and likely ecosystem CO_2 fluxes) varied among vegetation types at intermediate periods is a critical property that process-based ecosystem models should take into consideration. Our results showed that the relationships between P_s and soil moisture and soil temperature are dynamic and change along the frequency and time domains as discussed in the following two sections.

Wavelet coherence analysis: soil CO_2 production and soil water content

We used wavelet coherence analysis to quantify the degree of linear relationship between the nonstationary series of soil P_s and soil water content. Our results showed that the relationships between soil moisture and P_s were significant at intermediate periods (between 2- and 32-day), but were associated with discrete pulses in soil moisture (Fig. 4). The darker red areas inside the contour lines in Fig. 4 represent high local correlation between these two time series (representing 5% significance level; see 'Methods'), and the arrows indicate the phase relationship between these time series. Although we found a consistent correlation between P_s and soil moisture at intermediate periods (indicated by the *y*-axis), we found that the localization of these correlations varied in the time domain (represented by the *x*-axis) among vegetation types (Fig. 4).

In general, the local correlation (denoted by darker red areas in Fig. 4) was higher at mature woody vegetation than at the other vegetation types suggesting a strong link between variations in P_s and soil water content especially at the beginning of the winter rains (DOY 350 and 700 after January 1, 2006; Fig. 4a). In the young woody vegetation and herbaceous meadow, the effects of the summer rainfalls (DOY $\sim$ 200 and $\sim$ 600 after January 1, 2006) in soil water content appeared to be largely correlated with P_s (Fig. 4b and c). The different response to water pulses between vegetation types could be associated with differences in plant phenology, root biomass (Table 1), mycorrhizal strategy (Vargas & Allen, 2008b), or the ability of larger plants to tap groundwater (Querejeta *et al*., 2009) during the dry summer months by mature woody vegetation. At the herbaceous meadow we observed the importance of water pulses for P_s as seen in other herbaceous semiarid ecosystems (Huxman *et al*., 2004). With lower plant, fine roots, and rhizomorphs density, heterotrophic respiration is likely to be dependent on pulses of water input during warm conditions, where a large pool of readily digestible carbon may be rapidly consumed by the rehydrated microbial community (Fierer *et al*., 2003; Schimel *et al*., 2007).

Our results showed that P_s responded differently to variation in soil water content among vegetation types, and using wavelet coherence analysis we were able to

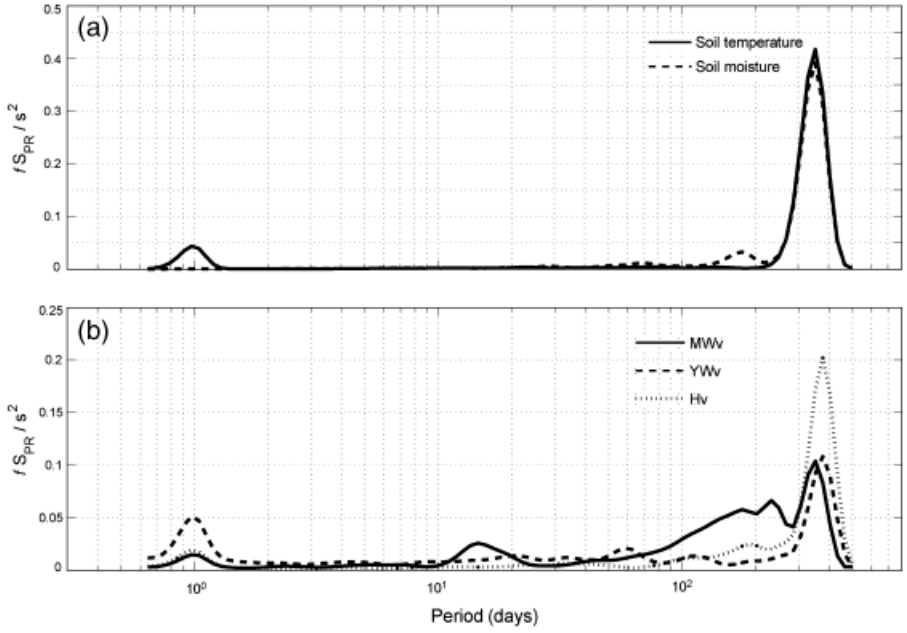

Fig. 3 Global wavelet power spectrum of (a) soil temperature and soil moisture, and (b) soil CO_2 production (P_s) at three vegetation types. MWv, mature woody vegetation; YWv, young woody vegetation; Hv, scattered herbaceous meadow.

identify significant correlations in frequency (*y*-axis) and time domains (*x*-axis; Fig. 4). These results could be applied for pulse responses analyses and models as we identified that the variation of P_s to the pulse is associated to specific periods between 2- and 32-days. Further rain pulse experiments could be design to identify processes that regulate the fluxes at those periods among different vegetation types, climate conditions, soil textures, and soil nutrient gradients.

Wavelet coherence analysis: soil CO_2 production and soil temperature

Wavelet coherence analysis was also applied to quantify the relationship between the time series of soil P_s and soil temperature. A strong significant local correlation was observed at the 1-day period (see dark red areas along the 1-day period in *y*-axis; Fig. 5) at all vegetation types as biological processes depend on diel temperature cycles (Fig. 3a). Noteworthy, the local correlation was substantial at the 1-day period for mature woody vegetation (Fig. 5a), while there was a wide range of periods that showed local correlation at the young woody vegetation and the scattered herbaceous meadow (Fig. 5b and c).

The local correlation at the meadow was stronger at the 4–64-day periods. These coherencies were significant during increasing temperatures under wet conditions during spring (Fig. 5c, DOY 100–200 and 400–500 after January 1, 2006). These local correlations were also observed during the same time of the year at young woody vegetation, but we also observed significant local correlations when soil moisture increased early in the fall (Fig. 5b, DOY 350 and 700 after January 1, 2006). The influence of changes in soil temperature on P_s at larger periods was more sensitive at herbaceous meadow where the vegetation cover is reduced as seen previously in grasslands (Bahn *et al.*, 2008). Furthermore, the local correlation between soil temperature and P_s was significant during conditions of high soil water content, suggesting the importance of temperature during these wet conditions. These results support the general observation that soil CO_2 fluxes are related to changes in soil temperature (Lloyd & Taylor, 1994), but we showed that these relationships vary in the frequency and time domains, likely as a result of changes in moisture availability and substrate supply (Davidson *et al.*, 2006).

Using wavelet coherence analysis one can extract phase relationships between two time series (represented as arrows in Figs 4 and 5), and this information could provide insights of biophysical controls on soil CO_2 fluxes (H2). To test this hypothesis we calculated the wavelet coherence between the time series of P_s and soil temperature, P_s, and PAR at the 1-day period to study diel responses.

Our results showed that lags between P_s and both soil temperature and PAR varied each day showing that there is not a constant diel lag for each vegetation type (Fig. 6). Overall we found that PAR increased 5 and 3 h before P_s at woody and herbaceous vegetation types,

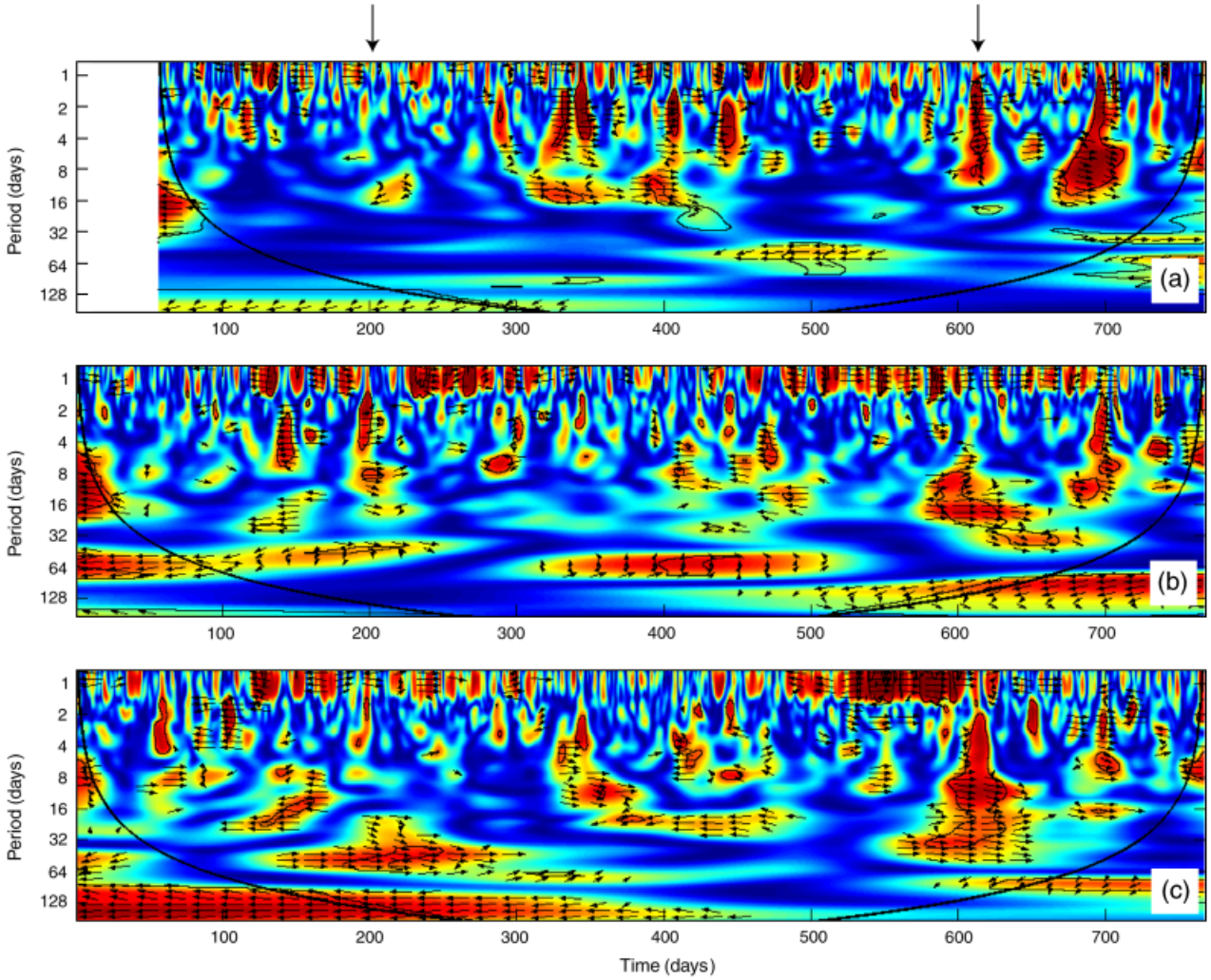

Fig. 4 Wavelet coherence analysis and phase difference between soil CO_2 production (P_s) and soil water content at (a) mature woody vegetation, (b) young woody vegetation, and (c) scattered herbaceous meadow from January 2006 to February 2008. The phase difference is shown by arrows: in-phase pointing right (no lags between time series), out of phase pointing in other direction (representing lags between time series). The color codes for power values are from dark blue (low values) to dark red (high values). Black contour lines represent the 5% significance level and thick black line indicates the cone of influence that delimits the region not influenced by edge effects. DOY, day of the year after January 1, 2006. Arrows at the top of the panels indicate the approximate date of summer rainfall events.

respectively. In contrast, soil temperature increased between 3 and 4 h after P_s at woody vegetation types, but soil temperature was in phase (no lags) with P_s at the herbaceous site. When comparing lags between these time series we found that variation in phase angles between P_s and PAR explains nearly 70% and 80% of the variation in phase angles between P_s and soil temperature ($P<0.001$) in woody vegetation sites (Fig. 6a and b). This was not the case for the scattered herbaceous meadow (Fig. 6c).

At woody vegetation sites nearly 62% of the measurements showed lags >1 h between P_s and both soil temperature and PAR (Fig. 6a and b). The relationship of lags between soil temperature and P_s was strongest during the spring when soil moisture was decreasing but temperature was increasing. Furthermore, early spring was also the time where lags between P_s and PAR explained the variation in lags between soil temperature and P_s (Fig. 6a and b). Our results suggest that at the 1-day period photosynthesis of woody vegetation is likely to precede soil CO_2 fluxes and support previous observations (Tang *et al*., 2005).

At herbaceous vegetation nearly 64% of the measured days had lags <1 h between P_s and soil temperature (at the 1-day period), but there was a more constant pattern of lags between P_s and PAR among days (Fig. 6c). These

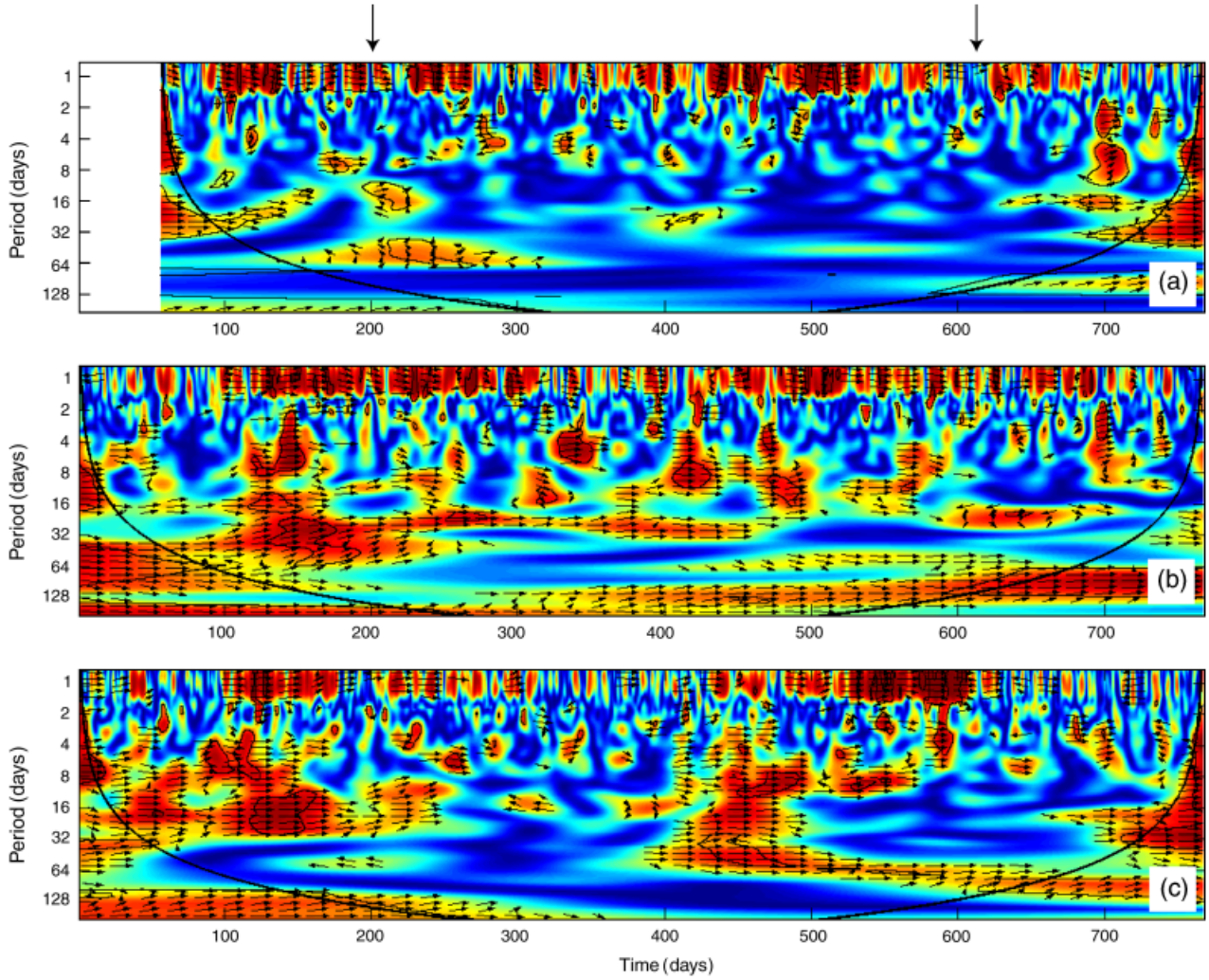

Fig. 5 Wavelet coherence analysis and phase difference between soil CO_2 production (*Ps*) and soil temperature at (a) mature woody vegetation, (b) young woody vegetation, and (c) herbaceous vegetation from January 2006 to February 2008. The phase difference is shown by arrows: in-phase pointing right (no lags between time series), out of phase pointing in other direction (representing lags between time series). The color codes for power values are from dark blue (low values) to dark red (high values). Black contour lines represent the 5% significance level and thick black line indicates the cone of influence that delimits the region not influenced by edge effects. DOY, day of the year after January 1, 2006. Arrows at the top of the panels indicate the approximate date of summer rainfall events.

results suggest that the biophysical mechanisms that regulate P_s are tightly coupled with the frequency of the soil temperature signal, and support previous observations that photosynthesis regulates R_s (at the 1-day period) by a rapid transfer of carbon for respiratory use in short stature vegetation (Carbone & Trumbore, 2007; Bahn *et al.*, 2009).

Our results support the fact that PAR (as a surrogate for photosynthesis) regulates soil CO_2 fluxes at the 1-day period at different vegetation types, but showed that this influence is not consistent with time. We propose that different mechanisms prevail under different weather, plant physiological, and soil conditions at the 1-day period. These results bring attention to the need for understanding the biophysical mechanisms that regulate the diel variation of lags between CO_2 fluxes and soil temperature, and PAR. Possible general mechanisms that influence the lags between these time series are (a) changes in soil CO_2 diffusivity; (b) daily variation in carbon phloem transport that may influence the transport to labile carbon to the root and the microbes (Thompson & Holbrook, 2004); (c) changes in heat transfer in the soil due to changes in soil moisture; and (d) changes in daily transport of dissolved CO_2 in the xylem among vegetation types (McGuire & Teskey, 2004). We propose that isotope

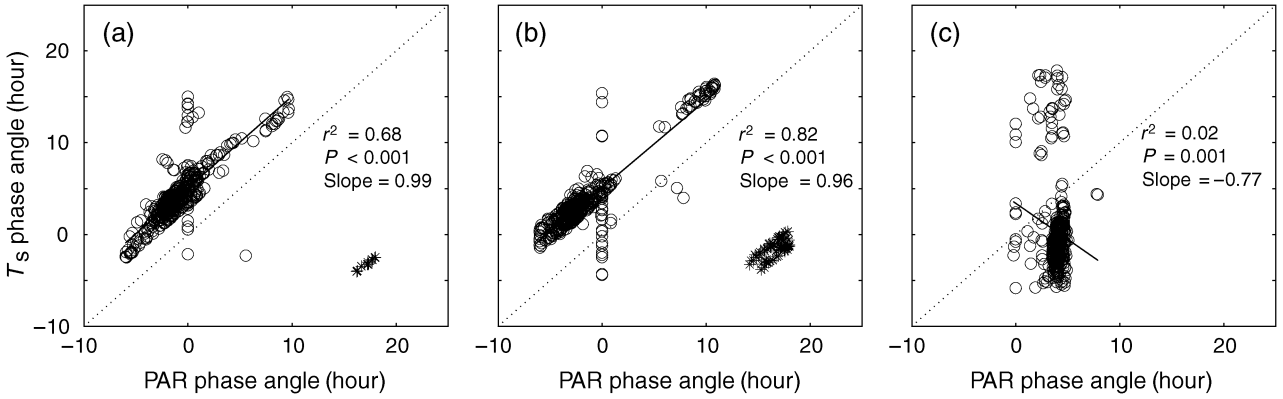

Fig. 6 Average phase difference (in hours) between soil CO_2 production (*Ps*) and soil temperature (T_s phase angle), and between P_s and photosynthetic active radiation (PAR phase angle) at (a) mature woody vegetation, (b) young woody vegetation, and (c) scattered herbaceous meadow. Average phase differences were calculated for the 1-day period when the wavelet coherence power was significant ($\alpha = 0.5$). Positive values mean that P_s precedes temperature or PAR. Open circles (○) represent days at the end of the rainy season and asterisks (*) represent days at the beginning of the rainy season. Data represented by an asterisk (*) were not included to calculate the linear regression statistics. Dashed line represents 1 : 1 line.

analysis for tracking the fate of carbon among vegetation types are an important complement to time series analysis to better understand the mechanisms that regulate the lags between environmental variables and soil CO_2 fluxes.

Our results were based on soil temperature measured at the soil depth (8 cm) where P_s was measured, but the interpretation of these results do not change using soil temperatures measured at different depths. The effect of heat transfer in the soil influenced the calculation of the phase angles among sites (Fig. 7), but because of the consistency on changes among vegetation types our conclusions are robust. However, it is critical to identify the depth of highest P_s to better associate a respective temperature with soil CO_2 processes (Pavelka *et al*., 2007). Future studies should identify the depth of maximum P_s in the soil profile, and explore which are the mechanisms that regulate the vertical distribution of production of CO_2 in the soil.

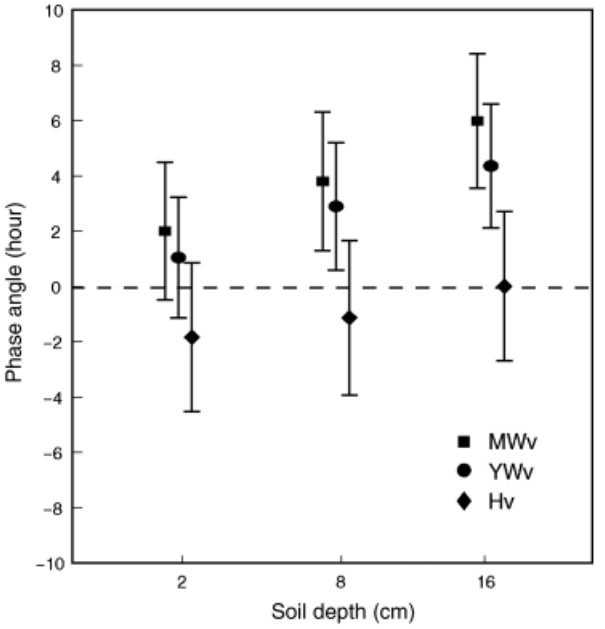

Fig. 7 Average phase difference (in hours) between soil CO_2 production (*Ps*) and soil temperature at 2, 8, and 16 cm depth for the 1-day period when the wavelet coherence power was significant ($\alpha = 0.5$). Positive values mean that P_s precedes temperature. Dashed line represents zero shift (i.e. no lag in hours) between variables.

Wavelet analysis and soil respiration modeling

Multiple empirical soil respiration models are based on variation in soil temperature and soil water content (e.g. Davidson *et al*., 1998; Reichstein *et al*., 2003), but their performance may vary depending on the frequency analyzed (e.g. using daily average or monthly average). Given the complexity of mechanisms involved in soil CO_2 processes, a first step is to reevaluate the performance of simple empirical models. Here we evaluated empirical models using inputs at 1-h intervals, and compared their performances in the frequency domain. We believe that a first step to improve model structure and model performance is first to identify were the models fail in both the frequency and time domains.

We analyzed two simple empirical models previously used in Mediterranean ecosystems (Xu *et al*., 2004; Vargas & Allen, 2008c) and selected the best fit based on the RMSE and the AIC (Table 3). We determined that an empirical model with soil temperature [Eqn (8),

Table 3 Nonlinear regression results relating soil CO_2 production to soil water content and soil temperature at three vegetation types at the James Reserve

Vegetation type	Model	B_1	B_2	B_3	B_4	r^2	RMSE	AIC
MWv	I	2.973	0.143	–	–	0.22	31.18	22.95
	II	0.059	0.235	5.107	792.247	0.36	28.45	21.64
YWv	I	8.002	0.041	–	–	0.24	7.76	20.65
	II	4.771	0.056	4.861	–18.601	0.31	7.42	18.65
Hv	I	4.817	0.043	–	–	0.40	4.17	17.5
	II	0.053	5.019	−16.734	0.053	0.44	4.02	19.5

Model I has the form $P_s = B_1 e^{(B_2 T)}$ and model II the form $P_s = B_1 e^{(B_2 T)} e^{(B_3 \theta) + (B_4 \theta^2)}$. The best-fit model parameters (B_1–B_4) are reported for each model together with the squared coefficient of regression (r^2), the RMSE and the AIC. T is temperature (°C) at 8 cm depth, θ is volumetric water content ($m^{-3}\,m^{-3}$), and P_s is soil CO_2 production (μmol $CO\,m^{-3}\,s^{-1}$). Model parameters were estimated using the Levenberg–Marquardt method. The models are fit with the hourly data in the three vegetation types.
AIC, Akaike Information Criterion; MWv, mature woody vegetation; RMSE, root mean-squared error; YWv, young woody vegetation; Hv, scattered herbaceous meadow.

model I] was the best fit for P_s in the scattered herbaceous meadow, whereas a model including soil temperature and soil moisture was the best to represent P_s at mature and young woody vegetation [Eqn (9), model II]. Using hourly data the r^2 values of the models were low ($r^2 < 0.5$, Table 3), but allowed us to represent variation of P_s at multiple periods (Fig. 8). We used the continuous wavelet transform on the residuals of the models to identify significant regions in the spectral signature where the error variance was significant (Fig. 8). Significant regions of error are represented by the red areas within the cone of influence in Fig. 8. The models failed to represent high-frequency (~1-day period) and low-frequency components (>36-day periods) for each vegetation type (see dark red areas inside contour lines). These results can be compared with the observations in the lack of coherence between soil temperature and moisture with P_s at similar periods (blue areas outside contour lines in Figs 4 and 5).

In mature woody vegetation the model failed to explain variation at 1-day period from DOY 150 to 240 and from DOY 550 to 600 (after January 1, 2006) as represented by the red areas inside the contour lines at the 1-day period (Fig. 8a). These results support the observations that other variables rather than soil temperature and soil water content would be needed to explain soil CO_2 fluxes at the study site (Vargas & Allen, 2008b). Noteworthy, the regions where the model failed were associated with periods of stress characterized by high temperatures and low soil water content (Fig. 1). The effect of the summer rainfall events can be seen at periods between 2- and 8-day. In addition, we found a significant large model failure between DOY 150 and 450 (after January 1, 2006) at periods between 8- and 128-day associated with large fluctuations of P_s during the wet spring conditions of the year of 2006 (Fig. 1).

In the young woody vegetation, the model failed to explain variation at periods larger than 4-day and especially over 64-day (red areas inside contour lines, Fig. 8b). In general, the model represented well the 1-day period except when soil water content increased during the summer rainfall events and during the winter rains. The effect of the summer rainfall can also be seen at periods between 2- and 8-day. The largest source of error was associated with low temperatures and high moisture content (DOY 350–450; after January 1, 2006), but the influence of seasonal precipitation on P_s was difficult to represent at >32-day periods. These results bring special attention to the role of water and temperature pulses and how to better understand their influence and prediction of soil CO_2 fluxes.

At the scattered herbaceous meadow, we used a simple exponential model using only soil temperature (Table 3), and this model accurately represented variation in P_s at most periods along the time domain. However, this model failed to explain variation at periods >32-day (red areas inside contour lines) mainly influenced by seasonal changes in soil water content (Fig. 8c). Noteworthy, this model accurately represents variation at 1-day period supporting the results that temperature is the main control of soil CO_2 fluxes in grassland sites (Bahn *et al*., 2009). The effect of the summer rainfall events can be seen at periods between 2- and 8-day and >32-day for the first year, but only at 16- and 32-day periods for the second year (Fig. 8).

It has been reported that terrestrial ecosystem models performed poorly in Mediterranean sites because of problems in the representation of water stress effects on CO_2 dynamics (Morales *et al*., 2005). Our results suggest that water stress effects are likely to influence the variance in P_s at intermediate periods (i.e. weeks to months), but we showed that the relationship

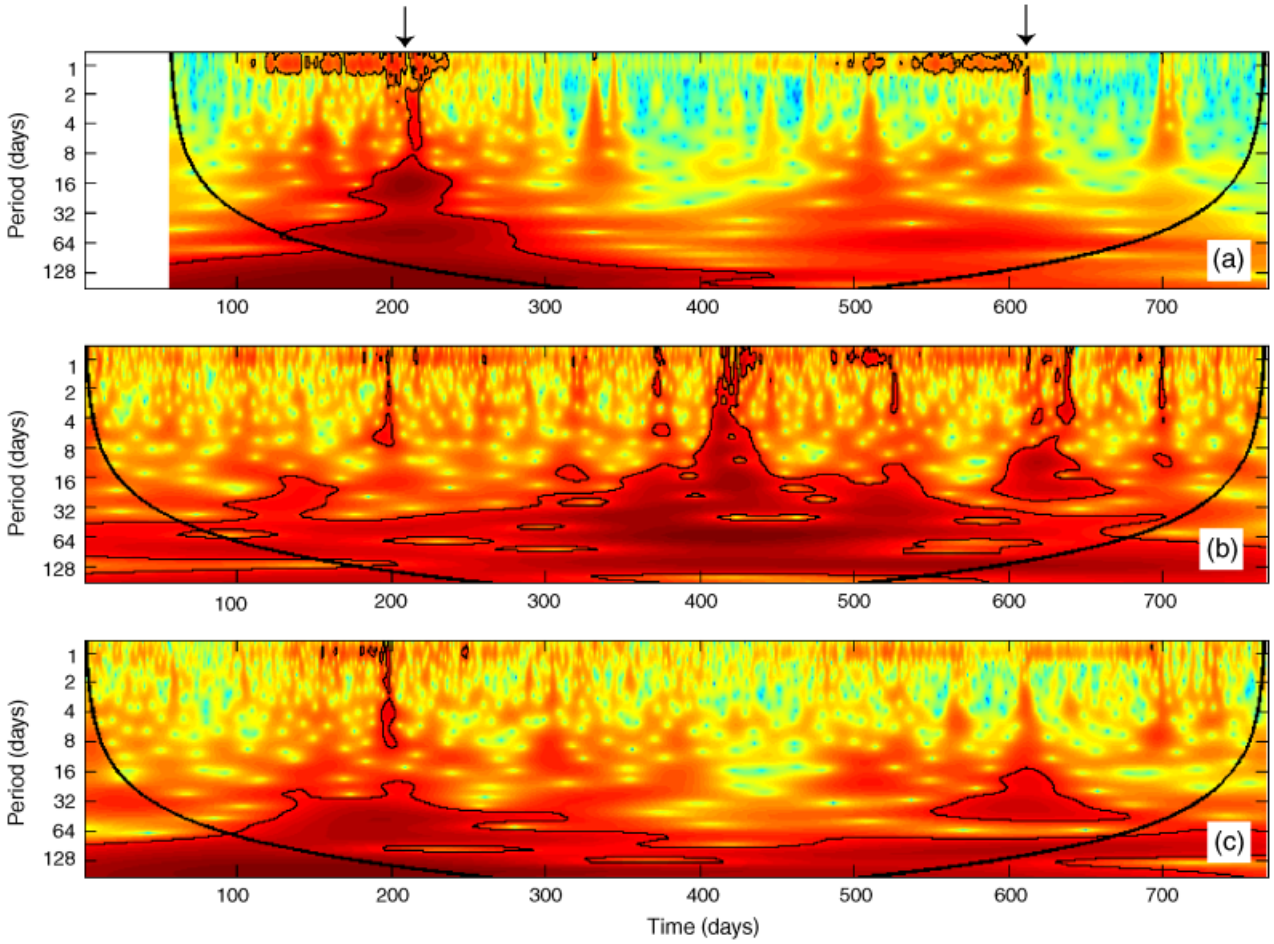

Fig. 8 Continuous wavelet power spectra for residuals of models for soil CO_2 production (*Ps*) at (a) mature woody vegetation, (b) young woody vegetation, and (c) herbaceous meadow from January 2006 to February 2008. The models used were selected based on the Akaike Information Criterion (AIC) and the root mean-squared error (see Table 3). The color codes for power values are from dark blue (low values) to dark red (high values). Black contour lines represent the 5% significance level and thick black line indicates the cone of influence that delimits the region not influenced by edge effects. DOY, day of the year after January 1, 2006. Arrows at the top of the panels indicate the approximate date of summer rainfall event.

between P_s and soil moisture is dynamic and change along the frequency and time domains. Thus, there is a need to integrate modeling and experimental efforts in water stressed systems to better understand biophysical processes that act at intermediate periods for better representation of CO_2 responses to weather variation.

Conclusions

Soil respiration processes are complex because the interactions between climatic forcing and biological components act at multiple temporal scales. In order to understand these interactions we used wavelet coherence analysis on continuous measurements of soil CO_2 production as a novel approach for terrestrial CO_2 flux research. The main advantage of wavelet coherence analysis approach is the ability to analyze transient dynamics for the association between two time series and the calculation of the phase difference. Our analysis has helped to identify repeating periods (i.e. hours, days, weeks, months, years) along the time domain (i.e. day of year) where different biophysical factors influence soil CO_2 fluxes. Our results provide several key points: first, rain pulses and rapid temperature changes influence soil CO_2 fluxes differently depending on the vegetation type. The influence of these water and temperature pulses can be seen at intermediate periods (e.g. weeks to months) in the frequency domain. Second, we propose that the information extracted from wavelet analysis is an alternative method for the under-

standing of biophysical frequency relations of soil CO_2 fluxes that have remained unclear so far. Here we showed that PAR (as a surrogate for photosynthesis) influenced soil CO_2 fluxes at the 1-day period but this influence is not consistent through time. Third, a first step to improve modeling of soil CO_2 fluxes is to evaluate model performances at multiple frequency and time domains. The temporal domains where the models fail provide information about biophysical processes that are not captured by these empirical models. Finally, we expect that time series analyses will become more common with increasing growth of continuous biometeorological measurements (e.g. ecosystem CO_2 fluxes, CH_4, NO_2, and O_3) by environmental networks such as the National Ecological Observatory Network (NEON), Integrated Carbon Observation System (ICOS), and FLUXNET.

Acknowledgements

This research was undertaken with funding from the National Science Foundation no. EF-0410408, the Center for Embedded Networked Sensing no. CCR-0120778, CONACyT, and the Kearney Foundation. R. V. was supported by grant DEB-0639235 while writing this manuscript.

References

Allen MF, Vargas R, Graham EA *et al*. (2007) Soil sensor technology: life within a pixel. *Bioscience*, **57**, 859–867.

Bachelet D, Neilson RP, Lenihan JM, Drapek RJ (2001) Climate change effects on vegetation distribution and carbon budget in the United States. *Ecosystems*, **4**, 164–185.

Bahn M, Rodeghiero M, Anderson-Dunn M *et al*. (2008) Soil respiration in european grasslands in relation to climate and assimilate supply. *Ecosystems*, **11**, 1352–1367.

Bahn M, Schmitt M, Siegwolf R, Richter A, Bruggemann N (2009) Does photosynthesis affect grassland soil-respired CO_2 and its carbon isotope composition on a diurnal timescale? *New Phytologist*, **182**, 451–460.

Baldocchi D, Falge E, Wilson K (2001) A spectral analysis of biosphere–atmosphere trace gas flux densities and meteorological variables across hour to multi-year time scales. *Agricultural and Forest Meteorology*, **107**, 1–27.

Baldocchi D, Tang JW, Xu LK (2006) How switches and lags in biophysical regulators affect spatial-temporal variation of soil respiration in an oak-grass savanna. *Journal of Geophysical Research*, **111**, G02008, doi: 10.1029/2005JG000063.

Battles JJ, Robards T, Das A, Waring K, Gilless JK, Biging G, Schurr F (2008) Climate change impacts on forest growth and tree mortality: a data-driven modeling study in the mixed-conifer forest of the Sierra Nevada, California. *Climatic Change*, **87**, S193–S213.

Bowling DR, McDowell NG, Bond BJ, Law BE, Ehleringer JR (2002) C-13 content of ecosystem respiration is linked to precipitation and vapor pressure deficit. *Oecologia*, **131**, 113–124.

Burnham KP, Anderson DR (2002) *Model Selection and Inference. A Practical Information-Theoretic Approach*. Springer, Berlin.

Carbone MS, Trumbore SE (2007) Contribution of new photosynthetic assimilates to respiration by perennial grasses and shrubs: residence times and allocation patterns. *New Phytologist*, **76**, 124–135.

Carbone MS, Winston GC, Trumbore SE (2008) Soil respiration in perennial grass and shrub ecosystems: linking environmental controls with plant and microbial sources on seasonal and diel timescales. *Journal of Geophysical Research*, G09022, doi: 09010.01029/02007JG000611.

Cazelles B, Chavez M, Berteaux D, Menard F, Vik JO, Jenouvrier S, Stenseth NC (2008) Wavelet analysis of ecological time series. *Oecologia*, **156**, 287–304.

Chen D, Molina JAE, Clapp CE, Venterea RT, Palazzo AJ (2005) Corn root influence on automated measurement of soil carbon dioxide concentrations. *Soil Science*, **170**, 779–787.

Collineau S, Brunet Y (1993) Detection of turbulent coherent motions in a forest canopy. 1. Wavelet analysis. *Boundary-Layer Meteorology*, **65**, 357–379.

Collins SL, Sinsabaugh RL, Crenshaw C, Green L, Porras-Alfaro A, Stursova M, Zeglin LH (2008) Pulse dynamics and microbial processes in arid land ecosystems. *Journal of Ecology*, **96**, 413–420.

Curiel Yuste J, Janssens IA, Carrara A, Meiresonne L, Ceulemans R (2003) Interactive effects of temperature and precipitation on soil respiration in a temperate maritime pine forest. *Tree Physiology*, **23**, 1263–1270.

Daly E, Oishi AC, Porporato A, Katul GG (2008) A stochastic model for daily subsurface CO_2 concentration and related soil respiration. *Advances in Water Resources*, **31**, 987–994.

Daubechies I (1990) The wavelet transform, time–frequency localization and signal analysis. *Ieee Transactions on Information Theory*, **36**, 961–1005.

Davidson EA, Belk E, Boone RD (1998) Soil water content and temperature as independent or confounded factors controlling soil respiration in a temperate mixed hardwood forest. *Global Change Biology*, **4**, 217–227.

Davidson EA, Janssens IA, Luo YQ (2006) On the variability of respiration in terrestrial ecosystems: moving beyond Q(10). *Global Change Biology*, **12**, 154–164.

Davidson EA, Trumbore SE (1995) Gas diffusivity and production of CO_2 in deep soils of the Eastern Amazon. *Tellus Series B-Chemical and Physical Meteorology*, **47**, 550–565.

Davidson EA, Verchot LV, Cattanio JH, Ackerman IL, Carvalho JEM (2000) Effects of soil water content on soil respiration in forests and cattle pastures of eastern Amazonia. *Biogeochemistry*, **48**, 53–69.

DeForest JL, Noormets A, McNulty SG, Sun G, Tenney G, Chen JQ (2006) Phenophases alter the soil respiration–temperature relationship in an oak-dominated forest. *International Journal of Biometeorology*, **51**, 135–144.

Diffenbaugh NS, Giorgi F, Pal JS (2008) Climate change hotspots in the United States. *Geophysical Research Letters*, **35**, L16709, doi: 10.1029/2008GL035075.

Drewitt GB, Black TA, Nesic Z *et al*. (2002) Measuring forest floor CO_2 fluxes in a Douglas-fir forest. *Agricultural and Forest Meteorology*, **110**, 299–317.

Farge M (1992) Wavelet transforms and their applications to turbulence. *Annual Review of Fluid Mechanics*, **24**, 395–457.

Fierer N, Allen AS, Schimel JP, Holden PA (2003) Controls on microbial CO_2 production: a comparison of surface and subsurface soil horizons. *Global Change Biology*, **9**, 1322–1332.

Gao W, Li BL (1993) Wavelet analysis of coherent structures at the atmosphere forest interface. *Journal of Applied Meteorology*, **32**, 1717–1725.

Gaumont-Guay D, Black AT, Griffis TJ, Barr AG, Jassal RS, Nesic Z (2006) Interpreting the dependence of soil respiration on soil temperature and water content in a boreal aspen stand. *Agricultural and Forest Meteorology*, **140**, 220–235.

Goulden ML, Crill PM (1997) Automated measurements of CO_2 exchange at the moss surface of a black spruce forest. *Tree Physiology*, **17**, 537–542.

Govindan RB, Raethjen J, Kopper F, Claussen JC, Deuschl G (2005) Estimation of time delay by coherence analysis. *Physica A*, **350**, 277–295.

Grinsted A, Moore JC, Jevrejeva S (2004) Application of the cross wavelet transform and wavelet coherence to geophysical time series. *Nonlinear Processes in Geophysics*, **11**, 561–566.

Hanson PJ, Edwards NT, Garten CT, Andrews JA (2000) Separating root and soil microbial contributions to soil respiration: a review of methods and observations. *Biogeochemistry*, **48**, 115–146.

Hashimoto S, Suzuki M (2002) Vertical distributions of carbon dioxide diffusion coefficients and production rates in forest soils. *Soil Science Society of America Journal*, **66**, 1151–1158.

Hudgins L, Friehe CA, Mayer ME (1993) Wavelet transforms and atmospheric-turbulence. *Physical Review Letters*, **71**, 3279–3282.

Hughes L (2000) Biological consequences of global warming: is the signal already apparent? *Trends in Ecology and Evolution*, **15**, 56–61.

Huxman TE, Snyder KA, Tissue D *et al*. (2004) Precipitation pulses and carbon fluxes in semiarid and arid ecosystems. *Oecologia*, **141**, 254–268.

IPCC (2007) Climate change 2007: the physical science basis. In: *Contribution of Working Group I to the Fourth Assessment Report of the Intergovernmental Panel on Climate Change* (eds Solomon S, Qin D, Manning M, Chen Z, Marquis M, Averyt KB, Tignor M and Miller HL), Cambridge University Press, Cambridge, UK, 996pp.

Irvine J, Law BE (2002) Contrasting soil respiration in young and old-growth ponderosa pine forests. *Global Change Biology*, **8**, 1183–1194.

Irvine J, Law BE, Martin JG, Vickers D (2008) Interannual variation in soil CO_2 efflux and the response of root respiration to climate and canopy gas exchange in mature ponderosa pine. *Global Change Biology*, **14**, 2848–2859.

Jarvis P, Rey A, Petsikos C *et al*. (2007) Drying and wetting of Mediterranean soils stimulates decomposition and carbon dioxide emission: the "Birch effect". *Tree Physiology*, **27**, 929–940.

Jassal R, Black A, Novak M, Morgenstern K, Nesic Z, Gaumont-Guay D (2005) Relationship between soil CO_2 concentrations and forest-floor CO_2 effluxes. *Agricultural and Forest Meteorology*, **130**, 176–192.

Katul G, Lai CT, Schafer K, Vidakovic B, Albertson J, Ellsworth D, Oren R (2001a) Multiscale analysis of vegetation surface fluxes: from seconds to years. *Advances in Water Resources*, **24**, 1119–1132.

Katul G, Vidakovic B, Albertson J (2001b) Estimating global and local scaling exponents in turbulent flows using discrete wavelet transformations. *Physics of Fluids*, **13**, 241–250.

Kumar P, Foufoula Georgiou E (1997) Wavelet analysis for geophysical applications. *Reviews of Geophysics*, **35**, 385–412.

Lau KM, Weng H (1995) Climate signal detection using wavelet transform: how to make a time series sing. *Bulletin of the American Meteorological Society*, **76**, 2391–2402.

Lenihan JM, Drapek R, Bachelet D, Neilson RP (2003) Climate change effects on vegetation distribution, carbon, and fire in California. *Ecological Applications*, **13**, 1667–1681.

Liu Q, Edwards NT, Post WM, Gu L, Ledford J, Lenhart S (2006) Temperature-independent diel variation in soil respiration observed from a temperate deciduous forest. *Global Change Biology*, **12**, 2136–2145.

Lloyd J, Taylor JA (1994) On the temperature dependence of soil respiration. *Functional Ecology*, **8**, 315–323.

Mahecha MD, Reichstein M, Lange H *et al*. (2007) Characterizing ecosystem-atmosphere interactions from short to interannual time scales. *Biogeosciences*, **4**, 743–758.

Maraun D, Kurths J (2004) Cross wavelet analysis: significance testing and pitfalls. *Nonlinear Processes in Geophysics*, **11**, 505–514.

McGuire MA, Teskey RO (2004) Estimating stem respiration in trees by a mass balance approach that accounts for internal and external fluxes of CO_2. *Tree Physiology*, **24**, 571–578.

Minnich RA, Barbour MG, Burk JH, Sosa-Ramirez J (2000) Californian mixed-conifer forests under unmanaged fire regimes in the sierra san Pedro Martir, Baja California, Mexico. *Journal of Biogeography*, **27**, 105–129.

Moldrup P, Olesen T, Yamaguchi T, Schjonning P, Rolston DE (1999) Modeling diffusion and reaction in soils. IX. The Buckingham–Burdine–Campbell equation for gas diffusivity in undisturbed soil. *Soil Science*, **164**, 542–551.

Morales P, Sykes MT, Prentice IC *et al*. (2005) Comparing and evaluating process-based ecosystem model predictions of carbon and water fluxes in major european forest biomes. *Global Change Biology*, **11**, 2211–2233.

Moren AS, Lindroth A (2000) CO_2 exchange at the floor of a boreal forest. *Agricultural and Forest Meteorology*, **101**, 1–14.

Pavelka M, Acosta M, Marek MV, Kutsch W, Janous D (2007) Dependence of the $Q(10)$ values on the depth of the soil temperature measuring point. *Plant and Soil*, **292**, 171–179.

Potts DL, Huxman TE, Enquist BJ, Weltzin JF, Williams DG (2006) Resilience and resistance of ecosystem functional response to a precipitation pulse in a semi-arid grassland. *Journal of Ecology*, **94**, 23–30.

Querejeta JI, Egerton-Warburton LM, Allen MF (2009) Topographic position modulates the mycorrhizal response of oak trees to interannual rainfall variability. *Ecology*, **90**, 649–662.

Raich JW, Potter CS (1995) Global patterns of carbon dioxide emissions from soils. *Global Biogeochemical Cycles*, **9**, 23–36.

Raich JW, Potter CS, Bhagawati D (2002) Interannual variability in global soil respiration, 1980–94. *Global Change Biology*, **8**, 800–812.

Reichstein M, Rey A, Freibauer A *et al*. (2003) Modeling temporal and large-scale spatial variability of soil respiration from soil water availability, temperature and vegetation productivity indices. *Global Biogeochemical Cycles*, **17**, 1104, doi: 10.1029/2003GB002035.

Riveros-Iregui DA, Emanuel RE, Muth DJ *et al*. (2007) Diurnal hysteresis between soil CO_2 and soil temperature is controlled by soil water content. *Geophysical Research Letters*, **34**, L17404, doi: 10.1029/2007GL030938.

Ryan MG, Law BE (2005) Interpreting, measuring, and modeling soil respiration. *Biogeochemistry*, **73**, 3–27.

Savage KE, Davidson EA (2003) A comparison of manual and automated systems for soil CO_2 flux measurements: trade-offs between spatial and temporal resolution. *Journal of Experimental Botany*, **54**, 891–899.

Schimel J, Balser TC, Wallenstein M (2007) Microbial stress-response physiology and its implications for ecosystem function. *Ecology*, **88**, 1386–1394.

Schimel JP, Clein JS (1996) Microbial response to freeze–thaw cycles in tundra and taiga soils. *Soil Biology and Biochemistry*, **28**, 1061–1066.

Šimůnek J, Suarez DL (1993) Modeling of carbon-dioxide transport and production in soil. 1. Model development. *Water Resources Research*, **29**, 487–497.

Stoy PC, Katul GG, Siqueira MBS *et al*. (2005) Variability in net ecosystem exchange from hourly to inter-annual time scales at adjacent pine and hardwood forests: a wavelet analysis. *Tree Physiology*, **25**, 887–902.

Stoy PC, Palmroth S, Oishi AC *et al*. (2007) Are ecosystem carbon inputs and outputs coupled at short time scales? A case study from adjacent pine and hardwood forests using impulse-response analysis. *Plant Cell and Environment*, **30**, 700–710.

Tang J, Baldocchi DD, Xu L (2005) Tree photosynthesis modulates soil respiration on a diurnal time scale. *Global Change Biology*, **11**, 1298–1304.

Thompson MV, Holbrook NM (2004) Scaling phloem transport: information transmission. *Plant Cell and Environment*, **27**, 509–519.

Torrence C, Compo GP (1998) A practical guide to wavelet analysis. *Bulletin of the American Meteorological Society*, **79**, 61–78.

Torrence C, Webster PJ (1999) Interdecadal changes in the enso-monsoon system. *Journal of Climate*, **12**, 2679–2690.

Vargas R, Allen MF (2008a) Diel patterns of soil respiration in a tropical forest after hurricane Wilma. *Journal of Geophysical Research-Biogeosciences*, **113**, G03021, doi: 10.1029/2007JG000620.

Vargas R, Allen MF (2008b) Dynamics of fine root, fungal rhizomorphs, and soil respiration in a mixed temperate forest: integrating sensors and observations. *Vadose Zone Journal*, **7**, 1055–1064.

Vargas R, Allen MF (2008c) Environmental controls and the influence of vegetation type, fine roots and rhizomorphs on diel and seasonal variation in soil respiration. *New Phytologist*, **179**, 460–471.

Xu LK, Baldocchi DD, Tang JW (2004) How soil moisture, rain pulses, and growth alter the response of ecosystem respiration to temperature. *Global Biogeochemical Cycles*, **18**, GB4002, doi: 10.1029/2004GB002281.